Efficient real-space approach to time-dependent density functional theory for the dielectric response of nonmetallic crystals

Kootstra, F.; de Boeij, P. L.; Snijders, J. G.

Published in:
Journal of Chemical Physics

DOI:
10.1063/1.481315

Efficient real-space approach to time-dependent density functional theory for the dielectric response of nonmetallic crystals

F. Kootstra, P. L. de Boeij, and J. G. Snijders
Theoretical Chemistry, Materials Science Centre, Rijksuniversiteit Groningen, Nijenborgh 4, 9747 AG Groningen, The Netherlands

(Received 3 November 1999; accepted 28 January 2000)

Time-dependent density functional theory has been used to calculate the static and frequency-dependent dielectric function $\epsilon(\omega)$ of nonmetallic crystals. We show that a real-space description becomes feasible for crystals by using a combination of a lattice-periodic (microscopic) scalar potential with a uniform (macroscopic) electric field as perturbation in a periodic structure calculation. The induced density and microscopic potential can be obtained self-consistently for fixed macroscopic field by using linear response theory in which Coulomb interactions and exchange-correlation effects are included. We use an iterative scheme, in which density and potential are updated in every cycle. The explicit evaluation of Kohn–Sham response kernels is avoided and their singular behavior as function of the frequency is treated analytically. Coulomb integrals are evaluated efficiently using auxiliary fitfunctions and we apply a screening technique for the lattice sums. The dielectric function can then be obtained from the induced current. We obtained $\epsilon(\omega)$ for C, Si, and GaAs within the adiabatic local density approximation in good agreement with experiment. In particular in the low-frequency range no adjustment of the local density approximation (LDA) band gap seems to be necessary. © *2000 American Institute of Physics.* [S0021-9606(00)31215-6]

I. INTRODUCTION

In the early 1960s Hohenberg and Kohn[1] formulated the fundamental theorems of density functional theory (DFT) for the description of the ground state of an interacting-electron system in an external potential. This theory proved to be very practical after Kohn and Sham[2] incorporated it in a one-electron self-consistent field calculation scheme (SCF). This method has nowadays become one of the standard tools for the first-principle calculation of the properties of solids,[3] and also for atoms and molecules.[4–6] The accuracy of the results obtained with these methods is very good for a wide variety of ground state properties of solids, atoms, and molecules. Amongst the exceptions the most prominent is the large deviation for the energy gap and the dielectric constant in semiconductors and insulators. The value for the dielectric constant obtained within the local density approximation (LDA) is usually much larger (more than 10%)[7,8] than the experimental data. A similar overestimation has been found for the static polarizabilities of atoms.[9] However, inclusion of the correct asymptotic behavior of the exchange-correlation potential[10] greatly improves the results for the atomic polarizabilities.[11] This correction, which is due to the contribution of the outer region, seems to be less important for molecules,[11] so we should not expect large deviations for the LDA results in solids either.

In solids the discrepancy for the dielectric constant is often attributed to the mismatch between the Kohn–Sham energy gap and the gap as observed in optical spectra. LDA typically underestimates the gap by 30%–50%. Attempts to improve these results by improving the quality of the various approximations for the exchange-correlation functional have had limited success. The inclusion of gradient corrections to the LDA reduces the error only slightly.[12,13] The error in the Kohn–Sham energy gap can be attributed to a discontinuity in the DFT exchange-correlation potential[14,15] and it is commonly believed that the gap has to be corrected by a rigid shift of the virtual states in order to get good results for the quasiparticle energies and dielectric constant.[8,16–18] There is however no formal justification within DFT for this so-called scissors operator.[13] In some materials, one has to use a different shift in order to match the excitation spectrum than to get a correct dielectric constant.[18] Gonze, Ghosez, and Godby[19] have indicated that this scissors-operator is an approximate way to deal with the special role of macroscopic polarization in these infinite systems. They made the remark that the original assumptions of Hohenberg and Kohn are no longer valid in these systems, and that in principle the density must be supplemented with the macroscopic polarization in order to describe these systems completely.

The time-dependent extension of DFT, (TDDFT) rigorously proven in the 1980s by Runge and Gross,[20] gave some new impetus to this field of research. Whereas ordinary DFT was formulated originally only for the nondegenerate ground state, Runge and Gross showed that the validity of the theorems could be extended to cover systems in time-dependent scalar potentials as well. The application of this theory to atoms and molecules proved to be very successful, e.g., the calculated response properties and excitation energies were greatly improved.[11,21–23] Ghosh and Dhara[24,25] showed that TDDFT also applies to systems which are being subjected to general time-dependent electromagnetic fields, in which case both the density and the current density are needed to fully

describe the system. We will follow their description and derive an expression for the macroscopic polarization from the current density.

Most implementations of TDDFT for solids use pseudopotentials in combination with a plane-wave basis.[7,8,16] This combination facilitates the description for the induced properties, like density and induced fields in Fourier space.[26,27] Self-consistency is achieved in a method which needs the construction of various response kernels as large matrix representations on this plane-wave basis, and for which one usually has to invert these matrices.[7,28] High accuracy can only be achieved at the expense of huge computation costs. We will show that a real-space description is possible, and we present a self-consistent field method, which is comparable in efficiency to ordinary ground-state calculations. This computational scheme is similar to the density-functional perturbation scheme of Baroni *et al.*[29] We extended the full-potential linear combination of atomic orbitals (LCAO) implementation (ADF-BAND)[30,31] for our response calculations, in which we achieve the same spatial resolution for the induced density as for the ground-state density. Coulomb interaction (local-field effects) and exchange-correlation effects have been fully included in this calculation scheme.

The outline of this article is as follows. First we give the derivation of the real-space description for crystalline systems. We make use of a separation into microscopic and macroscopic components for the potentials and fields, and we describe how they can be used in the time-dependent Kohn–Sham scheme. Then the main aspects of the implementation are given. We show how symmetry can be used to reduce the computational effort, and we explain the self-consistency procedure. Finally we demonstrate the method for the crystals of C, Si, and GaAs, and discuss the results.

II. THEORY

The theory of the dielectric properties of solids describes the linear response of crystals to externally applied electric fields. One of the central problems in this theory is how to model real systems that are large but nevertheless finite using idealized periodic crystals of infinite extent. One can only make this connection by considering the proper asymptotic limit of finite systems to infinite size. In this section we show that it is important to identify macroscopic and microscopic contributions to the electric field and polarization. For the finite system we have to do this in such a way that surface and sample-shape dependent contributions can be separated from the bulk-intrinsic parts.

Before we formulate our microscopic treatment, let us recall the definitions for the macroscopic electric field $\mathbf{E}_{\mathrm{mac}}(\mathbf{r},t)$ and the macroscopic polarization $\mathbf{P}_{\mathrm{mac}}(\mathbf{r},t)$. Without losing generality we can consider the time-dependence to be harmonic with frequency ω. One commonly defines the macroscopic field at a point $\mathbf{r}$ inside the bulk as the average field that a test charge would experience in a region $\Omega_{\mathbf{r}}$ surrounding the point $\mathbf{r}$. This region must have a size d that is small compared to the wavelength $\lambda = 2\pi c/\omega$, but it nevertheless has to contain a large number of bulk unit cells; i.e., for $\lambda \gg d \gg a$, where a is the lattice parameter, we can define

$$\mathbf{E}_{\mathrm{mac}}(\mathbf{r},t) = \frac{1}{|\Omega_{\mathbf{r}}|} \int_{\Omega_{\mathbf{r}}} (\mathbf{E}_{\mathrm{ext}}(\mathbf{r}',t) + \mathbf{E}_{\mathrm{ind}}(\mathbf{r}',t))\, d\mathbf{r}'. \tag{1}$$

This macroscopic field contains the externally applied electric field plus the macroscopic part of the induced field. This induced field is the result of the reaction of the system to the external field.

Similarly the induced macroscopic polarization can be defined as the time-integral of the average induced current flowing in this region $\Omega_{\mathbf{r}}$,

$$\mathbf{P}_{\mathrm{mac}}(\mathbf{r},t) = -\frac{1}{|\Omega_{\mathbf{r}}|} \int^{t} \int_{\Omega_{\mathbf{r}}} \delta\mathbf{j}(\mathbf{r}',t')\, d\mathbf{r}'\, dt', \tag{2}$$

where $\delta\mathbf{j}(\mathbf{r},t)$ is the induced current density. Note that the definition for the macroscopic polarization of Eq. (2) is valid in all systems. It only becomes equivalent to the more common notion of ''an induced average dipole moment per unit volume,'' i.e., to $-\int_{\Omega_{\mathbf{r}}} \mathbf{r}'\, \delta\rho(\mathbf{r}',t)\, d\mathbf{r}'/|\Omega_{\mathbf{r}}|$ when this property is properly defined. This is only the case in systems where we can define the volume $\Omega_{\mathbf{r}}$ such that no currents flow across its boundary.

Inside the bulk the macroscopic polarization is related to the macroscopic electric field rather than to the externally applied field, via what is called the constitutive equation

$$\mathbf{P}_{\mathrm{mac}}(\mathbf{r},t) = \int^{t} \chi_e(t-t') \cdot \mathbf{E}_{\mathrm{mac}}(\mathbf{r},t')\, dt'. \tag{3}$$

This equation defines the material property $\chi_e(\tau)$ called the electric susceptibility, from which the macroscopic dielectric function $\epsilon(\tau)$ is derived,

$$\epsilon(\tau) = 1 + 4\pi\chi_e(\tau). \tag{4}$$

In general $\chi_e(\tau)$ and $\epsilon(\tau)$ are tensors, which, however, simplify to scalars in isotropic systems.

In order to be able to derive these material properties, we have to give a microscopic account of the macroscopic contributions to the electric field and polarization for an arbitrary but fixed region $\mathcal{B}_{\mathbf{r}}$ inside the bulk. We therefore identify in the interior of the sample a large number of identical but otherwise arbitrary bulk unit cells, each having the same volume $|V|$. The cells which comprise the region $\mathcal{B}_{\mathbf{r}}$ will be enumerated using the indices i and are denoted by V_i.

Within the long-wavelength limit we can assume that in these cells both the induced charge and current distribution become lattice periodic. Hence the macroscopic field component becomes uniform throughout $\mathcal{B}_{\mathbf{r}}$. Under these conditions all relevant properties become lattice periodic and we can model the response of the region $\mathcal{B}_{\mathbf{r}}$ by using a model system with periodic boundary conditions.

However, we cannot obtain the electric field by simply evaluating the contributions of the lattice-periodic sources. Only the microscopic part can be obtained using the periodic lattice, since the macroscopic component depends also on the external field and the sample shape, which are no longer properly defined in the periodic—hence infinite—model system. Instead we can consider the uniform macroscopic field for the periodic model system to be fixed. We will now construct the microscopic and macroscopic (scalar and vector)

potentials which are due to the induced sources, and we will show that they lead to microscopic and macroscopic fields, respectively.

For any finite region Ω we can define the scalar potential $\delta v(\mathbf{r},t)$ of the induced density $\delta\rho(\mathbf{r},t)=\rho(\mathbf{r},t)-\rho_0(\mathbf{r})$. The action is instantaneous within the Coulomb gauge, so the potential follows from [we will use atomic units ($e=\hbar=m=1$) throughout this article]

$$\delta v(\mathbf{r},t)=\int_\Omega \frac{\delta\rho(\mathbf{r}',t)}{|\mathbf{r}-\mathbf{r}'|}d\mathbf{r}'. \tag{5}$$

It is well-established that this potential is not properly defined in the limit of $|\Omega|$ to infinite size. In the periodic model system this ambiguity arises due to the divergent and conditionally convergent lattice sum contributions of the monopole, dipole, and quadrupole moments of the density in the cells V_i.

We can, however, define the microscopic component of this Coulomb potential by removing these conditionally convergent contributions. Therefore we construct for each unit cell V_i a uniform monopole, dipole, and quadrupole density, and we subtract their contributions $\delta v_i(\mathbf{r},t)$ from the bare Coulomb potential of Eq. (5) according to

$$\delta v_{\mathrm{mic}}(\mathbf{r},t)=\sum_i \left(\int_{V_i} \frac{\delta\rho(\mathbf{r}',t)}{|\mathbf{r}-\mathbf{r}'|}d\mathbf{r}' - \delta v_i(\mathbf{r},t)\right). \tag{6}$$

The summation is over all cells V_i in the region $\mathcal{B}_\mathbf{r}$. The potential $\delta v_i(\mathbf{r},t)$ is defined as

$$\delta v_i(\mathbf{r},t)=\int_{V_i}\sum_{n=0}^{2}\frac{1}{n!}\delta\mu^{(n)}_{i,j_1\cdots j_n}(t)\cdot\frac{\partial}{\partial r'_{j_1}}\cdots\frac{\partial}{\partial r'_{j_n}} \times\frac{1}{|\mathbf{r}-\mathbf{r}'|}d\mathbf{r}'. \tag{7}$$

In this expression we have implied a summation over all Cartesian components j_1 through j_n of the uniform multipole density of rank n, which are denoted by $\delta\mu_i^{(n)}(t)$. These uniform densities have to be constructed carefully in order to ensure that the conditionally convergent terms of Eq. (5) are exactly canceled in Eq. (6). Their value can be obtained for each cell V_i by requiring that all three lowest-order terms in the multipole expansion of the contribution of this cell to the microscopic potential of Eq. (6) must vanish. The expansion can be taken with respect to an arbitrary origin $\mathbf{R}_i$ inside V_i. The monopole density has to vanish in the periodic system due to the condition of charge neutrality. One can easily check that the uniform dipole and quadrupole densities can then be obtained from the average dipole and quadrupole moments of the unit cells. If we choose to represent these moments with respect to the geometric centers, i.e., with respect to $\mathbf{R}_i=(1/|V|)\int_{V_i}\mathbf{r}'\,d\mathbf{r}'$, we obtain for this particular choice

$$\delta\mu_i^{(n)}(t)=\frac{1}{|V|}\int_{V_i}\delta\rho(\mathbf{r}',t)(\mathbf{r}'-\mathbf{R}_i)^n\,d\mathbf{r}', \tag{8}$$

where on the right-hand side the nth tensor product is meant. Due to the periodicity these multipole densities are identical for each cell, so we can drop the index i in the sequel. By removing the conditionally convergent terms in this way, the series of Eq. (6) becomes nicely convergent. If we choose $\mathcal{B}_\mathbf{r}$ finite but nevertheless sufficiently large, so that convergence is reached within $\mathcal{B}_\mathbf{r}$, we have established a proper definition for the microscopic potential for both periodic and finite systems.

On the other hand, the macroscopic potential can only be defined for the true, finite system. It forms the remainder of the bare Coulomb potential after the microscopic part has been removed. The terms $\delta v_i(\mathbf{r},t)$ (which were not included in the microscopic contribution of region $\mathcal{B}_\mathbf{r}$) have to be included in the macroscopic part of the potential

$$\delta v_{\mathrm{mac}}(\mathbf{r},t)=\int{}'\frac{\delta\rho(\mathbf{r}',t)}{|\mathbf{r}-\mathbf{r}'|}d\mathbf{r}'+\sum_i \delta v_i(\mathbf{r},t). \tag{9}$$

Here the integration domain in the first term on the right-hand side is the whole (finite) system, however, with the exclusion of the region $\mathcal{B}_\mathbf{r}$. This is indicated by the prime on the integral sign. The contribution of $\mathcal{B}_\mathbf{r}$ is given by the potential of the uniform multipole densities. Note that the resulting macroscopic potential comprises all surface and sample-shape dependent contributions, but excludes the microscopic contributions from the region $\mathcal{B}_\mathbf{r}$.

The uniform dipole and quadrupole sources in the region $\mathcal{B}_\mathbf{r}$ can equally well be represented using surface excess monopole and dipole layers at the boundary of $\mathcal{B}_\mathbf{r}$. Being remote, these can only lead to smooth, i.e., macroscopic fields at $\mathbf{r}$. A similar analysis holds for a uniform density in $\mathcal{B}_\mathbf{r}$. Although this density has to vanish in the periodic model system, a macroscopic density fluctuation on a wavelength scale can exist in the finite system, but it also can lead to only macroscopic fields. The microscopic potential, on the other hand, is lattice periodic, and can only lead to microscopic fields.

The nice result of this separation into microscopic and macroscopic contributions is that we are now able to evaluate the microscopic component of the Coulomb potential using the periodic model system. The summation of Eq. (6) is nicely convergent, since remote cells do not contribute. For its evaluation we can make use of a screening technique. Therefore, we introduce an envelope function which weighs the contributions of the individual cells such that it leaves nearby cells unchanged, but removes remote cells explicitly. This can be achieved using a spherically symmetric function $h_c(r)$ which is a smooth function of just the distance of the origin of the cells to the coordinate at which to evaluate the potential. This function is characterized by some cutoff radius c for the screening. The limiting case, where this cutoff radius is infinite automatically yields the correct (unscreened) value,

$$\delta v_{\mathrm{mic}}(\mathbf{r},t)=\lim_{c\to\infty}\sum_i h_c(|\mathbf{r}-\mathbf{R}_i|) \times\left(\int_{V_i}\frac{\delta\rho(\mathbf{r}',t)}{|\mathbf{r}-\mathbf{r}'|}d\mathbf{r}'-\delta v_i(\mathbf{r},t)\right). \tag{10}$$

We can separate the two contributions into two separately converging series. The screened potential of the periodic density can be evaluated efficiently, whereas the screened uniform multipole densities lead to a mere (time-dependent) uniform contribution (see Appendix A). The latter contribution can always be chosen to vanish by a suitable gauge transformation. We obtain

$$\delta v_{\mathrm{mic}}(\mathbf{r},t)=\lim_{c\to\infty}\left(\sum_i h_c(|\mathbf{r}-\mathbf{R}_i|)\int_{V_i}\frac{\delta\rho(\mathbf{r}',t)}{|\mathbf{r}-\mathbf{r}'|}d\mathbf{r}'\right). \tag{11}$$

In practice the convergence can be quite fast for suitably chosen screening functions such that the numerical evaluation of it can be very efficient.

The time-dependent induced density is not the only source of the electromagnetic fields. In large systems, the induced current density also contributes considerably. Therefore, we also have to consider the induced vector potential $\delta\mathbf{A}(\mathbf{r},t)$ which is defined within the Coulomb gauge according to

$$\delta\mathbf{A}(\mathbf{r},t)=\frac{1}{c}\int\frac{\delta\mathbf{j}_T(\mathbf{r}',t-|\mathbf{r}-\mathbf{r}'|/c)}{|\mathbf{r}-\mathbf{r}'|}d\mathbf{r}'. \tag{12}$$

Here $\delta\mathbf{j}_T(\mathbf{r},t)$ is the induced transverse current density. This vector potential accounts, apart from the properly retarded contribution of the total induced current, also for the retardation effects which have not been included in the instantaneous Coulomb potential.[32] We can safely neglect the effect of retardation in the microscopic part of the scalar potential which is due to the nearby surrounding only, but we cannot do this for the macroscopic part. This part also contains contributions from remote regions. As we did for the density and the Coulomb potential, we have to distinguish microscopic and macroscopic contributions of the induced current density to this vector potential. We can safely ignore the microscopic part, because its electric field contribution is already a factor ω^2/c^2 in order smaller than that of the microscopic Coulomb potential. We will only have to retain the macroscopic part. This part is sample-shape dependent just like the macroscopic scalar potential.

We obtain the total macroscopic field from

$$\mathbf{E}_{\mathrm{mac}}(\mathbf{r},t)=\mathbf{E}_{\mathrm{ext}}(\mathbf{r},t)-\frac{1}{c}\frac{\partial}{\partial t}\delta\mathbf{A}_{\mathrm{mac}}(\mathbf{r},t)+\nabla\delta v_{\mathrm{mac}}(\mathbf{r},t). \tag{13}$$

Here all macroscopic retardation effects are properly accounted for. The microscopic contribution to the field is completely described using the instantaneous microscopic Coulomb potential. This potential is lattice periodic and can therefore not contain any components that represent a macroscopic electric field. The field $\mathbf{E}_{\mathrm{mac}}(\mathbf{r},t)$ of Eq. (13) is therefore indeed the macroscopic field of Eq. (1).

We can now define a new gauge which we will call the microscopic Coulomb gauge. In this gauge the new scalar potential $\Phi'(\mathbf{r},t)$ is given by the instantaneous microscopic potential $\delta v_{\mathrm{mic}}(\mathbf{r},t)$ of Eq. (11), while the associated vector potential $\mathbf{A}'(\mathbf{r},t)$ is fully retarded and completely specified by the macroscopic electric field $\mathbf{E}_{\mathrm{mac}}(\mathbf{r},t)$ of Eq. (13)

$$\Phi'(\mathbf{r},t)=-\delta v_{\mathrm{mic}}(\mathbf{r},t), \tag{14}$$

$$\mathbf{A}'(\mathbf{r},t)=-c\int^t\mathbf{E}_{\mathrm{mac}}(\mathbf{r},t')\,dt'. \tag{15}$$

In the definition of these potentials we have neglected the microscopic retardation and microscopic magnetic effects. This is consistent with the neglect of the Breit corrections[33] in ground-state calculations.

The problems posed by the sample-shape dependence of the macroscopic field are circumvented by prescribing the total macroscopic electric field in the bulk as being uniform. We explicitly leave the surface region and sample shape undefined. We then only have to obtain the microscopic Coulomb potential of the periodic system in order to completely describe the fields in the bulk region. The main conclusion of this analysis is that in the long-wavelength limit it suffices to know the induced lattice-periodic density and the induced macroscopic current density in the bulk for a given uniform macroscopic electric field in order to obtain the bulk-intrinsic induced microscopic potential and macroscopic polarization.

We can now treat the dynamic linear response of a crystal to a fixed macroscopic field, within the idealized periodic boundary approximation. We use the perturbation approach to time-dependent density functional theory (TDDFT), in which both scalar and vector potentials are used to describe the perturbation. In its most general form this theory states that all observable quantities are functionals of both the time-dependent particle density $\rho(\mathbf{r},t)$ and the current density $\mathbf{j}(\mathbf{r},t)$. Ghosh and Dhara[25] have shown that this time-dependent density and current density can be constructed using a generalization of the effective one-electron scheme of Kohn and Sham.[2] In this scheme the single-particle wave functions $\psi_n(\mathbf{r},t)$ are solutions of the following time-dependent Schrödinger-type equation,

$$i\frac{\partial}{\partial t}\psi_n(\mathbf{r},t)=\left(\frac{1}{2}\left|-i\nabla+\frac{1}{c}\mathbf{A}_{\mathrm{eff}}(\mathbf{r},t)\right|^2+v_{\mathrm{eff}}(\mathbf{r},t)\right)\psi_n(\mathbf{r},t), \tag{16}$$

for suitably chosen initial conditions. The particles move in time-dependent effective potentials $\{v_{\mathrm{eff}}(\mathbf{r},t),\mathbf{A}_{\mathrm{eff}}(\mathbf{r},t)\}$, which are uniquely determined (apart from an arbitrary gauge transform) by the exact time-dependent density and current density. These exact time-dependent densities follow from the solutions $\psi_n(\mathbf{r},t)$ via

$$\rho(\mathbf{r},t)=\sum_{n=1}^N|\psi_n(\mathbf{r},t)|^2, \tag{17}$$

and

$$\mathbf{j}(\mathbf{r},t)=\sum_{n=1}^N\Re\{-i\psi_n^*(\mathbf{r},t)\nabla\psi_n(\mathbf{r},t)\}-\frac{1}{c}\rho(\mathbf{r},t)\mathbf{A}_{\mathrm{eff}}(\mathbf{r},t). \tag{18}$$

The first and second term on the right-hand side of Eq. (18) are the paramagnetic and diamagnetic currents respectively.

The initial ground-state configuration is obtained by occupying only those one-electron states, which have evolved from the N solutions that are lowest in energy for the stationary state.

The effective potentials are the result of the externally applied potentials supplemented by internal contributions of the density and current density. These internal contributions comprise the classical potentials due the density and current density, in addition to contributions that account for the exchange and correlation effects. These exchange-correlation contributions are universal functionals of the density and current density. Like in the original Kohn–Sham scheme, these effective potentials have to be obtained self-consistently.

As we argued above, we choose to work in the microscopic Coulomb gauge, also for the effective potentials. We then have to split the exchange-correlation contributions into microscopic and macroscopic components. We will assume that the microscopic component of the exchange-correlation scalar potential is a functional of the periodic density alone, so that the effective microscopic scalar potential takes the following form:

$$v_{\mathrm{eff}}(\mathbf{r},t)=v_{\mathrm{mic}}(\mathbf{r},t)+v_{\mathrm{xc,mic}}[\rho](\mathbf{r},t). \tag{19}$$

For the microscopic xc potential we will use the same functional dependence on the periodic density as in the ground-state calculation, which is known as the adiabatic approximation. Again we will neglect any microscopic component of the effective vector potential. Moreover, all macroscopic components of the exchange-correlation contribution, which could give rise to a macroscopic exchange-correlation electric field,

$$\mathbf{E}_{\mathrm{xc,mac}}(\mathbf{r},t)=-\frac{1}{c}\frac{\partial}{\partial t}\mathbf{A}_{\mathrm{xc,mac}}(\mathbf{r},t)+\nabla v_{\mathrm{xc,mac}}(\mathbf{r},t), \tag{20}$$

will not be taken into account in the sequel. The effective vector potential becomes entirely defined by the macroscopic electric field via Eq. (15),

$$\mathbf{A}_{\mathrm{eff}}(\mathbf{r},t)=\mathbf{A}'(\mathbf{r},t)=-c\int^{t}\mathbf{E}_{\mathrm{mac}}(\mathbf{r},t')dt'. \tag{21}$$

With both effective potentials $v_{\mathrm{eff}}(\mathbf{r},t)$ and $\mathbf{A}_{\mathrm{eff}}(\mathbf{r},t)$ now properly defined, this completes the time-dependent self-consistency scheme.

For the calculation of linear response properties we only need to treat the time-dependent components of the density, current density, and potentials as first-order perturbations. First we obtain the ground-state density $\rho_0(\mathbf{r})$ and the ground-state effective scalar potential $v_{\mathrm{eff},0}(\mathbf{r})$ of this generalized Kohn–Sham problem. In the absence of any time-dependent macroscopic field this is an ordinary ground-state calculation. We then define the perturbation of the ground-state density by $\delta\rho(\mathbf{r},t)=\rho(\mathbf{r},t)-\rho_0(\mathbf{r})$. The change in the effective scalar potential $\delta v_{\mathrm{eff}}(\mathbf{r},t)=v_{\mathrm{eff}}(\mathbf{r},t)-v_{\mathrm{eff},0}(\mathbf{r})$ comprises two contributions,

$$\delta v_{\mathrm{eff}}(\mathbf{r},t)=\delta v_{\mathrm{mic}}(\mathbf{r},t)+\delta v_{\mathrm{xc}}[\rho](\mathbf{r},t). \tag{22}$$

The classical part of this potential, i.e., the induced microscopic scalar potential $\delta v_{\mathrm{mic}}(\mathbf{r},t)$, follows directly from Eq. (11). The first-order correction to the exchange-correlation potential, $\delta v_{\mathrm{xc}}[\rho](\mathbf{r},t)$, is formally defined using the (universal) exchange-correlation kernel $f_{\mathrm{xc}}(\mathbf{r},t;\mathbf{r}',t')$,

$$\delta v_{\mathrm{xc}}[\rho](\mathbf{r},t)=\int^{t}\int f_{\mathrm{xc}}[\rho_0](\mathbf{r},t;\mathbf{r}',t')\times\delta\rho(\mathbf{r}',t')\,d\mathbf{r}'\,dt'. \tag{23}$$

This kernel is the functional derivative of the time-dependent $v_{\mathrm{xc}}[\rho](\mathbf{r},t)$ with respect to the time-dependent density $\rho(\mathbf{r}',t')$. In this article we apply the adiabatic local-density approximation (ALDA) for the exchange-correlation kernel,

$$f_{\mathrm{xc}}^{\mathrm{ALDA}}[\rho_0](\mathbf{r},\mathbf{r}',t-t')=\delta(t-t')\frac{\partial v_{\mathrm{xc}}^{\mathrm{LDA}}[\rho_0](\mathbf{r})}{\partial\rho_0(\mathbf{r}')}=\delta(t-t')\,\delta(\mathbf{r}-\mathbf{r}')\times\frac{d^2(\rho\epsilon_{\mathrm{xc}}^{\mathrm{hom}}(\rho))}{d\rho^2}\Big|_{\rho=\rho_0(\mathbf{r})}, \tag{24}$$

where the exchange-correlation energy density $\epsilon_{\mathrm{xc}}^{\mathrm{hom}}(\rho)$ of the homogeneous electron gas is modeled using the Vosko–Wilk–Nussair[34] parametrization.

The induced density has to be obtained self-consistently. We do this in an iterative way, in which the macroscopic field $\mathbf{E}_{\mathrm{mac}}(t)$ is kept fixed while the induced effective potential $\delta v_{\mathrm{eff}}(\mathbf{r},t)$ is updated in each cycle using the perturbed density of the previous cycle. This procedure is repeated until it converged sufficiently.

The perturbation of the ground state which is due to the presence of the fixed uniform electric field and the induced scalar potential is governed by the perturbation Hamiltonian $\delta\hat{h}_{\mathrm{eff}}$, which is given by

$$\delta\hat{h}_{\mathrm{eff}}(\mathbf{E}_{\mathrm{mac}},\mathbf{r},t)=-\int^{t}\hat{\mathbf{j}}\cdot\mathbf{E}_{\mathrm{mac}}(t')\,dt'+\delta v_{\mathrm{eff}}(\mathbf{r},t). \tag{25}$$

Here only terms linear in the field have been retained. This perturbation is no longer a simple multiplicative operator like in ordinary TDDFT, since the macroscopic field couples to the (paramagnetic) current operator. This operator is defined as $\hat{\mathbf{j}}=-i(\nabla-\nabla^{\dagger})/2$, where the dagger indicates that terms to the left have to be differentiated. It is more convenient to go to the frequency domain to obtain an expression for the perturbed density. Using linear response theory, we get the induced density in first order,

$$\delta\rho(\mathbf{r},\omega)=\int\left(\frac{i}{\omega}\chi_{\rho\mathbf{j}}(\mathbf{r},\mathbf{r}',\omega)\cdot\mathbf{E}_{\mathrm{mac}}(\omega)+\chi_{\rho\rho}(\mathbf{r},\mathbf{r}',\omega)\,\delta v_{\mathrm{eff}}(\mathbf{r}',\omega)\right)d\mathbf{r}', \tag{26}$$

where the Kohn–Sham response functions $\chi_{\rho\rho},\chi_{\rho\mathbf{j}}(\mathbf{r},\mathbf{r}',\omega)$ are properties of the ground state. For periodic systems the ground-state solutions are characterized by Bloch functions $\psi_{n\mathbf{k}}$ having energies $\epsilon_{n\mathbf{k}}$. They are counted by their integer band index n and continuous Bloch vector $\mathbf{k}$ which is restricted to the first Brillouin zone V_{BZ}. The various response kernels $\chi_{ab}(\mathbf{r},\mathbf{r}',\omega)$ can be obtained from the following expression:

$$\chi_{ab}(\mathbf{r},\mathbf{r}',\omega)=\frac{1}{V_{\mathrm{BZ}}}\sum_{n,n'}\int_{V_{\mathrm{BZ}}}(f_{n\mathbf{k}}-f_{n'\mathbf{k}})\times\frac{(\psi^*_{n\mathbf{k}}(\mathbf{r})\,\hat{a}\,\psi_{n'\mathbf{k}}(\mathbf{r}))(\psi^*_{n'\mathbf{k}}(\mathbf{r}')\,\hat{b}\,\psi_{n\mathbf{k}}(\mathbf{r}'))}{\epsilon_{n\mathbf{k}}-\epsilon_{n'\mathbf{k}}+\omega+i\eta}d\mathbf{k}, \tag{27}$$

by substituting either $\hat{\rho}=1$ or $\hat{\mathbf{j}}=-i(\nabla-\nabla^{\dagger})/2$ for the operators $\hat{a}$ and $\hat{b}$. Here $f_{n\mathbf{k}}$ are the occupation numbers of the Bloch functions in the ground-state configuration. The positive infinitesimal η results from the adiabatic onset of the perturbation. Note that, since the perturbations are all lattice periodic, we only have to include those contributions in the response kernel that conserve the Bloch vector $\mathbf{k}$.

The induced current density can be obtained as soon as self-consistency is established. Correct up to first order we obtain an expression similar to Eq. (26),

$$\delta\mathbf{j}(\mathbf{r},\omega)=\int\left(\frac{i}{\omega}(\chi_{\mathbf{jj}}(\mathbf{r},\mathbf{r}',\omega)+\rho_0(\mathbf{r})\,\delta(\mathbf{r}-\mathbf{r}'))\cdot\mathbf{E}_{\mathrm{mac}}(\omega)+\chi_{\mathbf{j}\rho}(\mathbf{r},\mathbf{r}',\omega)\,\delta v_{\mathrm{eff}}(\mathbf{r}',\omega)\right)d\mathbf{r}', \tag{28}$$

where it is important to note that the macroscopic field also contributes in first order via the diamagnetic contribution to the current, $\mathbf{j}_d(\mathbf{r},\omega)=i\rho_0(\mathbf{r})\mathbf{E}_{\mathrm{mac}}(\omega)/\omega$. This contribution can be related to the static Kohn–Sham current–current response function, $\chi_{\mathbf{jj}}(\mathbf{r},\mathbf{r}',0)$ using the conductivity sum rule

$$[\chi_{\mathbf{jj}}(\mathbf{r},\mathbf{r}',0)]_{ij}+\rho_0(\mathbf{r})\,\delta_{ij}\delta(\mathbf{r}-\mathbf{r}')=0. \tag{29}$$

Note also that

$$\chi_{\mathbf{j}\rho}(\mathbf{r},\mathbf{r}',0)=0. \tag{30}$$

The induced current density is lattice-periodic, so that the macroscopic polarization is uniform and can be obtained from either Eq. (2) or (3) in their Fourier representations,

$$\mathbf{P}_{\mathrm{mac}}(\omega)=\chi_e(\omega)\cdot\mathbf{E}_{\mathrm{mac}}(\omega)=\frac{i}{V\omega}\int_V\delta\mathbf{j}(\mathbf{r},\omega)\,d\mathbf{r}. \tag{31}$$

During the SCF cycles we can set the macroscopic field to $\mathbf{E}_{\mathrm{mac}}(\omega)=-i\omega\,\mathbf{e}_j$, i.e., to a field linear in ω and directed along a unit vector $\mathbf{e}_j$ and thus avoid the singularities at $\omega=0$ in Eq. (26) and Eq. (28). Note that $\mathbf{E}_{\mathrm{mac}}(\omega)=\mathbf{E}^*_{\mathrm{mac}}(-\omega)$, so that this choice represents a real-valued electric field. This particular choice is equivalent to choosing a frequency-independent value for the vector potential, $\mathbf{A}'(\omega)=\mathbf{e}_j$. The diamagnetic contribution to the total induced current density of Eq. (28) then becomes frequency-independent, and, by using the special values for the static Kohn–Sham response functions of Eqs. (29) and (30), we obtain

$$\begin{aligned}\delta\mathbf{j}(\mathbf{r},\omega)&=\delta\mathbf{j}_p(\mathbf{r},\omega)+\delta\mathbf{j}_d(\mathbf{r},\omega)\\&=\delta\mathbf{j}_p(\mathbf{r},\omega)+\delta\mathbf{j}_d(\mathbf{r},0)\\&=\delta\mathbf{j}_p(\mathbf{r},\omega)-\delta\mathbf{j}_p(\mathbf{r},0).\end{aligned} \tag{32}$$

The Cartesian components of the susceptibility then follow from Eq. (31)

$$[\chi_e(\omega)]_{ij}=\left\{-\frac{1}{V\omega^2}\int_V[\,\delta\mathbf{j}_p(\mathbf{r},\omega)-\delta\mathbf{j}_p(\mathbf{r},0)]_i\,d\mathbf{r}\right\}_{\mathbf{E}_{\mathrm{mac}}(\omega)=-i\omega\,\mathbf{e}_j}. \tag{33}$$

There is a definite numerical advantage in rewriting the expression in this way. The diamagnetic and paramagnetic parts are treated on equal footing, hence a proper behavior for the static limit $\omega\to0$ is established.

III. IMPLEMENTATION

In this section we describe the main aspects of the implementation of the previously outlined method for TDDFT in crystalline systems. We will first discuss the role of symmetry in reducing the amount of computational effort. This has some important implications for the way the response calculations have been implemented.

The set of inhomogeneous linear transformations $\{\hat{\alpha}|\mathbf{t}_\alpha\}\mathbf{r}=\alpha\cdot\mathbf{r}+\mathbf{t}_\alpha$ that leave the crystal invariant constitutes the space group $\mathcal{G}$ of the crystal. Here α is a 3×3 rotation matrix, and $\mathbf{t}_\alpha$ a translation vector. The rotation parts $\hat{\alpha}$ separately form a finite group of order n_G, which is referred to as the point group G of the crystal. For clarity we will not consider the consequences of time-reversal symmetry here, and we will limit the discussion to the space-group elements only.

For a given macroscopic perturbing field $\mathbf{E}(\omega)$ of frequency ω we get an induced density at position $\mathbf{r}$ given by $\delta\rho(\mathbf{E},\mathbf{r},\omega)$. Here we have included the field as a parameter for notational convenience. Due to linearity we can treat the response to the Cartesian components of the field separately, and we get

$$\delta\rho(\mathbf{E},\mathbf{r},\omega)=\delta\rho\left(\sum_i E_i\,\mathbf{e}_i,\mathbf{r},\omega\right)=\sum_i E_i\,\delta\rho(\mathbf{e}_i,\mathbf{r},\omega). \tag{34}$$

The $\mathbf{e}_i$ are unit vectors in each of the three Cartesian directions. We can now define a vector field $\delta\boldsymbol{\rho}(\mathbf{r},\omega)$ by specifying its ith Cartesian component as the response to an electric field $\mathbf{E}(\omega)=-i\omega\,\mathbf{e}_i$, in the following way:

$$\delta\boldsymbol{\rho}(\mathbf{r},\omega)=\sum_i\,\delta\rho(-i\omega\,\mathbf{e}_i,\mathbf{r},\omega)\,\mathbf{e}_i. \tag{35}$$

For arbitrary given field $\mathbf{E}(\omega)$ the induced density then follows from Eq. (34),

$$\delta\rho(\mathbf{E},\mathbf{r},\omega)=\frac{i}{\omega}\,\delta\boldsymbol{\rho}(\mathbf{r},\omega)\cdot\mathbf{E}(\omega). \tag{36}$$

Under the application of a general rotation–translation $\{\hat{\alpha}|\mathbf{t}_\alpha\}$ this vector field transforms by definition as

$$\{\hat{\alpha}|\mathbf{t}_\alpha\}\,\delta\boldsymbol{\rho}(\mathbf{r},\omega)=\alpha\cdot\delta\boldsymbol{\rho}(\{\hat{\alpha}|\mathbf{t}_\alpha\}^{-1}\mathbf{r},\omega). \tag{37}$$

By subsequently substituting the definition of $\delta\boldsymbol{\rho}(\mathbf{r},\omega)$ of Eq. (35) and by applying the linearity property of Eq. (34) we obtain

$$\begin{aligned}\{\hat{\alpha}|\mathbf{t}_\alpha\}\,\delta\boldsymbol{\rho}(\mathbf{r},\omega) &= \sum_{ij}\ \alpha_{ji}\,\delta\rho(-i\omega\,\mathbf{e}_i,\{\hat{\alpha}|\mathbf{t}_\alpha\}^{-1}\mathbf{r},\omega)\,\mathbf{e}_j \\ &= \sum_{j}\ \delta\rho\Big(-i\omega\sum_i\ \alpha_{ji}\,\mathbf{e}_i,\{\hat{\alpha}|\mathbf{t}_\alpha\}^{-1}\mathbf{r},\omega\Big)\,\mathbf{e}_j \\ &= \sum_{j}\ \delta\rho(-i\omega\,\alpha^{-1}\cdot\mathbf{e}_j,\{\hat{\alpha}|\mathbf{t}_\alpha\}^{-1}\mathbf{r},\omega)\,\mathbf{e}_j\,.\end{aligned}$$

If $\{\hat{\alpha}|\mathbf{t}_\alpha\}$ is a symmetry operation of the crystal, then a rotated electric field $\alpha^{-1}\cdot\mathbf{e}_j$ gives the same response at the rotated point $\{\hat{\alpha}|\mathbf{t}_\alpha\}^{-1}\mathbf{r}$ as the original field $\mathbf{e}_j$ did at the original point $\mathbf{r}$. Hence we have

$$\begin{aligned}\{\hat{\alpha}|\mathbf{t}_\alpha\}\,\delta\boldsymbol{\rho}(\mathbf{r},\omega) &= \sum_{j}\ \delta\rho(-i\omega\,\alpha^{-1}\cdot\mathbf{e}_j,\{\hat{\alpha}|\mathbf{t}_\alpha\}^{-1}\mathbf{r},\omega)\,\mathbf{e}_j \\ &= \sum_{j}\ \delta\rho(-i\omega\,\mathbf{e}_j,\mathbf{r},\omega)\,\mathbf{e}_j=\delta\boldsymbol{\rho}(\mathbf{r},\omega),\end{aligned} \tag{38}$$

which proves that $\delta\boldsymbol{\rho}(\mathbf{r},\omega)$ transforms as a fully symmetric vector field under the operations of the crystal space group.

A similar analysis holds for the induced effective potential $\delta v_{\mathrm{eff}}(\mathbf{E},\mathbf{r},\omega)$, and we can introduce the vector field $\delta\mathbf{v}_{\mathrm{eff}}(\mathbf{r},\omega)$ accordingly, by an equation similar to Eq. (35),

$$\delta\mathbf{v}_{\mathrm{eff}}(\mathbf{r},\omega)=\sum_i\ \delta v_{\mathrm{eff}}(-i\omega\,\mathbf{e}_i,\mathbf{r},\omega)\,\mathbf{e}_i\,, \tag{39}$$

such that we have

$$\delta v_{\mathrm{eff}}(\mathbf{E},\mathbf{r},\omega)=\frac{i}{\omega}\,\delta\mathbf{v}_{\mathrm{eff}}(\mathbf{r},\omega)\cdot\mathbf{E}(\omega). \tag{40}$$

Note that, due to the totally-symmetric vector transformation property, we will have to evaluate these induced vector fields only for the irreducible wedge of the Wigner–Seitz cell.

We can now inspect that our formulas for the induced density indeed reflect these symmetry properties. By inserting the expression for the Kohn–Sham response kernels from Eq. (27) into the expression for the induced density from Eq. (26), we obtain

$$\delta\rho(\mathbf{E},\mathbf{r},\omega)=\frac{1}{V_{\mathrm{BZ}}}\sum_{n,n'}\ \int_{\mathrm{BZ}}\psi^*_{n\mathbf{k}}(\mathbf{r})\,\psi_{n'\mathbf{k}}(\mathbf{r}) \times\frac{(f_{n\mathbf{k}}-f_{n'\mathbf{k}})M_{n'n\mathbf{k}}(\mathbf{E},\omega)}{(\epsilon_{n\mathbf{k}}-\epsilon_{n'\mathbf{k}})+\omega+i\,\eta}\,d\mathbf{k}, \tag{41}$$

where the matrix elements $M_{n'n\mathbf{k}}$ are defined by

$$M_{n'n\mathbf{k}}(\mathbf{E},\omega)=\int\ \psi^*_{n'\mathbf{k}}(\mathbf{r}')\Big(\frac{i}{\omega}\,\hat{\mathbf{j}}\cdot\mathbf{E}(\omega) + \delta v_{\mathrm{eff}}(\mathbf{r}',\omega)\Big)\,\psi_{n\mathbf{k}}(\mathbf{r}')\,d\mathbf{r}'. \tag{42}$$

It immediately becomes clear that we do not have to evaluate and store the Kohn–Sham response kernels explicitly. Instead, we can obtain the induced density directly for any given perturbation, by evaluating these matrix elements separately.

The transformation properties of the Bloch functions enable us to limit the integration to the irreducible wedge of the Brillouin zone only. Since we do not consider the consequences of time-reversal symmetry here, the irreducible part is taken with respect to the crystal point group only. In a general $\mathbf{k}$-point we have the following transformation relation for any element $\{\hat{\alpha}|\mathbf{t}_\alpha\}$ of the space group:

$$\psi_{n\alpha\cdot\mathbf{k}}(\mathbf{r})=\exp(i\,\phi_{n\mathbf{k}}(\{\hat{\alpha}|\mathbf{t}_\alpha\}))\,\psi_{n\mathbf{k}}(\{\hat{\alpha}|\mathbf{t}_\alpha\}^{-1}\mathbf{r}). \tag{43}$$

Here $\phi_{n\mathbf{k}}(\{\hat{\alpha}|\mathbf{t}_\alpha\})$ is a real-valued function of $\mathbf{k}$ which depends on the particular band index and operator. Since $\psi_{n\mathbf{k}}(\mathbf{r})$ always occurs in Eq. (41) in combination with its complex conjugate via $M_{n'n\mathbf{k}}(\mathbf{E},\omega)$, this phase factor is irrelevant for our calculations. The occupation numbers $f_{n\mathbf{k}}$ are obtained in the ground-state configuration and are therefore functions of just the Kohn–Sham energy $\epsilon_{n\mathbf{k}}$. Since the energy transforms as $\epsilon_{n\alpha\cdot\mathbf{k}}=\epsilon_{n\mathbf{k}}$, we also have $f_{n\alpha\cdot\mathbf{k}}=f_{n\mathbf{k}}$. Hence both $f_{n\mathbf{k}}$ and $\epsilon_{n\mathbf{k}}$ are fully symmetric under the operations of the point group.

We can split the summation over the band indices n,n' into two parts, which involve only combinations of occupied with virtual states. Furthermore, we split the integration domain into equivalent wedges, which are related through the n_G operators $\hat{\alpha}$ of the point group. We obtain

$$\delta\rho(\mathbf{E},\mathbf{r},\omega)=\frac{1}{n_G V_{\mathrm{IBZ}}}\sum_{\hat{\alpha}\in G}\ \sum_{i}^{\mathrm{occ}}\ \sum_{a}^{\mathrm{virt}}\ \int_{\mathrm{IBZ}}\psi^*_{i\alpha\cdot\mathbf{k}}(\mathbf{r})\,\psi_{a\alpha\cdot\mathbf{k}}(\mathbf{r}) \times\frac{(f_{i\mathbf{k}}-f_{a\mathbf{k}})M_{ai\alpha\cdot\mathbf{k}}(\mathbf{E},\omega)}{(\epsilon_{i\mathbf{k}}-\epsilon_{a\mathbf{k}})+\omega+i\,\eta}\,d\mathbf{k}+\mathrm{c.c.}(-\omega). \tag{44}$$

The second part is the complex conjugate of the first part in which we have to replace ω by $-\omega$. This simple relation between the two parts is due to the fact that both $\mathbf{E}(t)$ and $v_{\mathrm{eff}}(\mathbf{r},t)$ have to be real-valued, such that $M_{ia\mathbf{k}}(\mathbf{E},\omega)=M^*_{ai\mathbf{k}}(\mathbf{E}^*,-\omega)$. Using the transformation rules of Eq. (43) for the wave functions $\psi_{n\alpha\cdot\mathbf{k}}(\mathbf{r})$, we can interchange the action of the symmetry operators between the reciprocal and real space. For the matrix elements we then get the following result:

$$M_{ai\alpha\cdot\mathbf{k}}(\mathbf{E},\omega)=\int\ \psi^*_{a\mathbf{k}}(\{\hat{\alpha}|\mathbf{t}_\alpha\}^{-1}\mathbf{r}')\Big(\frac{i}{\omega}\,\hat{\mathbf{j}}\cdot\mathbf{E}(\omega) + \delta v_{\mathrm{eff}}(\mathbf{r}',\omega)\Big)\,\psi_{i\mathbf{k}}(\{\hat{\alpha}|\mathbf{t}_\alpha\}^{-1}\mathbf{r}')\,d\mathbf{r}', \tag{45}$$

where we have dropped the phase factor of the transformation rule, as was argued above. By substituting $\mathbf{r}''=\{\hat{\alpha}|\mathbf{t}_\alpha\}^{-1}\mathbf{r}'$ and by making use of the vector transformation properties of both the current operator $\hat{\mathbf{j}}$ and the potential vector $\delta\mathbf{v}_{\mathrm{eff}}(\mathbf{r}',\omega)$ we obtain

$$M_{ai\alpha\cdot\mathbf{k}}(\mathbf{E},\omega)=\frac{i}{\omega}(\alpha\cdot\mathbf{M}_{ai\mathbf{k}}(\omega))\cdot\mathbf{E}(\omega), \tag{46}$$

with the vector $\mathbf{M}_{ai\mathbf{k}}(\omega)$ being given by

$$\mathbf{M}_{ai\mathbf{k}}(\omega)=\int \psi^*_{a\mathbf{k}}(\mathbf{r}'')(\hat{\mathbf{j}}+\delta\mathbf{v}_{\mathrm{eff}}(\mathbf{r}'',\omega))\psi_{i\mathbf{k}}(\mathbf{r}'')\,d\mathbf{r}''. \quad (47)$$

Substituting this result in Eq. (44) and applying again the transformation rule Eq. (43) yields the final result for the induced density. This density is fully specified by the vector density $\delta\boldsymbol{\rho}(\mathbf{r},\omega)$, which can be obtained as the totally-symmetric component of the auxiliary vector field $\delta\tilde{\boldsymbol{\rho}}(\mathbf{r},\omega)$ following

$$\delta\boldsymbol{\rho}(\mathbf{r},\omega)=\frac{1}{n_G}\sum_{\hat{\alpha}\in G}\{\hat{\alpha}|\mathbf{t}_\alpha\}\delta\tilde{\boldsymbol{\rho}}(\mathbf{r},\omega)+\mathrm{c.c.}(-\omega), \quad (48)$$

where we have defined $\delta\tilde{\boldsymbol{\rho}}(\mathbf{r},\omega)$ as

$$\delta\tilde{\boldsymbol{\rho}}(\mathbf{r},\omega)=\frac{1}{V_{\mathrm{IBZ}}}\sum_{i}^{\mathrm{occ}}\sum_{a}^{\mathrm{virt}}\int_{\mathrm{IBZ}}\psi^*_{i\mathbf{k}}(\mathbf{r})\psi_{a\mathbf{k}}(\mathbf{r}) \times\frac{(f_{i\mathbf{k}}-f_{a\mathbf{k}})\mathbf{M}_{ai\mathbf{k}}(\omega)}{(\epsilon_{i\mathbf{k}}-\epsilon_{a\mathbf{k}})+\omega+i\eta}d\mathbf{k}. \quad (49)$$

The integrations over the irreducible wedge of the Brillouin zone are evaluated numerically, by including the energy denominator into the integration weights of the quadrature

$$\frac{1}{V_{\mathrm{IBZ}}}\int_{\mathrm{IBZ}}\frac{(f_{i\mathbf{k}}-f_{a\mathbf{k}})}{(\epsilon_{i\mathbf{k}}-\epsilon_{a\mathbf{k}})+\omega+i\eta}g(\mathbf{k})\,d\mathbf{k} =\sum_{\mathbf{k}_j}w_{ia\mathbf{k}_j}(\omega)g(\mathbf{k}_j). \quad (50)$$

This way, the singular denominator can be handled analytically. The way these weights are obtained is the subject of Appendix B.

The induced density can now be used to evaluate the exchange-correlation potential using Eq. (23), which reduces in the ALDA approximation to the following simple relation:

$$\delta\mathbf{v}_{\mathrm{xc}}(\mathbf{r},\omega)=f_{\mathrm{xc}}^{\mathrm{ALDA}}[\rho_0](\mathbf{r})\;\delta\boldsymbol{\rho}(\mathbf{r},\omega). \quad (51)$$

The evaluation of the screened Coulomb potential becomes tractable by using auxiliary fitfunctions in a procedure similar to the one which was used in the ground-state calculation.[30] These fitfunctions have to be constructed in such a way that they reflect the symmetry transformation properties of the induced density. We therefore construct a set of real-valued vector functions $\{\mathbf{f}_i\}$, which transform as totally-symmetric vector fields

$$\mathbf{f}_i(\mathbf{r})=\{\hat{\alpha}|\mathbf{t}_\alpha\}\mathbf{f}_i(\mathbf{r})=\alpha\cdot\mathbf{f}_i(\{\hat{\alpha}|\mathbf{t}_\alpha\}^{-1}\mathbf{r}), \quad (52)$$

and for which the screened Coulomb integrals can be evaluated analytically. Thus we obtain for each function $\mathbf{f}_i(\mathbf{r})$ a potential function $\mathbf{g}_i(\mathbf{r})$ using Eq. (11),

$$\mathbf{g}_i(\mathbf{r})=\lim_{c\to\infty}\sum_j h_c(|\mathbf{r}-\mathbf{R}_j|)\int_{V_j}\frac{\mathbf{f}_i(\mathbf{r}')}{|\mathbf{r}-\mathbf{r}'|}d\mathbf{r}'. \quad (53)$$

The first-order density change $\delta\boldsymbol{\rho}(\mathbf{r},\omega)$ can then be represented on this basis of vector functions, using frequency-dependent coefficients $c_i(\omega)$,

$$\delta\boldsymbol{\rho}(\mathbf{r},\omega)=\sum_i c_i(\omega)\,\mathbf{f}_i(\mathbf{r}). \quad (54)$$

The coefficients $c_i(\omega)$ are fitted under the constraint that the net charge vanishes, which can be achieved automatically if none of the fitfunctions contains charge. This constraint is necessary to ensure that the microscopic potential actually exists. We obtain

$$\delta\mathbf{v}_{\mathrm{eff}}(\mathbf{r},\omega)=\sum_i c_i(\omega)\,\mathbf{g}_i(\mathbf{r})+\delta\mathbf{v}_{\mathrm{xc}}(\mathbf{r},\omega). \quad (55)$$

The way in which these fitfunctions can be constructed and the implementation of the constraint are the subject of Appendix C.

The self-consistent field scheme is now complete. Given a start-up value for the induced effective potential [e.g., $\delta\mathbf{v}_{\mathrm{eff}}(\mathbf{r},\omega)=\mathbf{0}$ for the uncoupled case], we can obtain the matrix elements for the perturbation from Eq. (47), and, with them, the induced density from Eq. (49) and Eq. (48). Using the fitting procedure, we obtain the new Coulomb contribution to the effective potential, and, from the density itself, the exchange-correlation contribution, Eq. (51) and Eq. (55). This completes the first cycle of the SCF scheme, and we iterate until convergence is reached. As convergence criterion we use the maximum change in the fitting coefficients for subsequent cycles, which must become negligible in order to reach convergence. The efficiency of this SCF procedure is increased by using the DIIS method (direct inversion of the iterative space) of Pulay.[35] The efficiency can be improved even further by using the converged result of a nearby frequency as start-up value for the calculation at the frequency at hand. Typically, convergence is reached in a few cycles.

With the converged results for the induced density and potential we can use the matrix elements of the SCF perturbation of Eq. (47) again to obtain the induced current density. We will only need to consider the paramagnetic part for the evaluation of the susceptibility. Similar to the definitions of the totally-symmetric density vector and potential vector, we define a tensor $\delta\mathcal{J}_p(\mathbf{r},\omega)$, by

$$\delta\mathcal{J}_p(\mathbf{r},\omega)=\sum_i\;\delta\mathbf{j}_p(-i\omega\,\mathbf{e}_i,\mathbf{r},\omega)\otimes\mathbf{e}_i, \quad (56)$$

so that we can obtain the induced paramagnetic current density from

$$\delta\mathbf{j}_p(\mathbf{E},\mathbf{r},\omega)=\frac{i}{\omega}\delta\mathcal{J}_p(\mathbf{r},\omega)\cdot\mathbf{E}(\omega). \quad (57)$$

In an analogous way as was proven for vector quantities, one easily verifies that this tensor transforms as a totally-symmetric tensor field,

$$\delta\mathcal{J}_p(\mathbf{r},\omega)=\{\hat{\alpha}|\mathbf{t}_\alpha\}\delta\mathcal{J}_p(\mathbf{r},\omega) =\alpha\cdot\delta\mathcal{J}_p(\{\hat{\alpha}|\mathbf{t}_\alpha\}^{-1}\mathbf{r},\omega)\cdot\alpha^{-1}. \quad (58)$$

The paramagnetic current density is obtained as the totally-symmetric part of the auxiliary tensor function $\delta\tilde{\mathcal{J}}_p(\mathbf{r},\omega)$, via

$$\delta\mathcal{J}_p(\mathbf{r},\omega)=\frac{1}{n_G}\sum_{\hat{\alpha}\in G}\{\hat{\alpha}|\mathbf{t}_\alpha\}\delta\tilde{\mathcal{J}}_p(\mathbf{r},\omega)+\text{c.c.}(-\omega), \quad (59)$$

in which we have defined $\delta\tilde{\mathcal{J}}_p(\mathbf{r},\omega)$ as

$$\delta\tilde{\mathcal{J}}_p(\mathbf{r},\omega)=\frac{-i}{2V_{\text{IBZ}}}\sum_{i}^{\text{occ}}\sum_{a}^{\text{virt}}\int_{\text{IBZ}}(\psi^*_{i\mathbf{k}}(\mathbf{r})\nabla\psi_{a\mathbf{k}}(\mathbf{r}) - \nabla\psi^*_{i\mathbf{k}}(\mathbf{r})\psi_{a\mathbf{k}}(\mathbf{r}))\frac{(f_{i\mathbf{k}}-f_{a\mathbf{k}})\mathbf{M}_{ai\mathbf{k}}(\omega)}{(\epsilon_{i\mathbf{k}}-\epsilon_{a\mathbf{k}})+\omega+i\eta}d\mathbf{k}. \quad (60)$$

The susceptibility then follows from Eq. (33) as

$$\chi_e(\omega)=\frac{-1}{\omega^2 V}\int_V(\delta\mathcal{J}_p(\mathbf{r},\omega)-\delta\mathcal{J}_p(\mathbf{r},0))\,d\mathbf{r}. \quad (61)$$

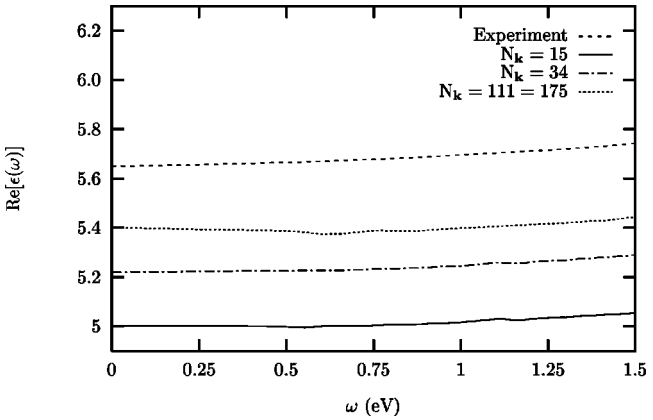

FIG. 1. The dielectric function for diamond in the low frequency range, obtained for various **k**-space samplings. The experimental data is taken from Ref. 39.

IV. RESULTS AND DISCUSSION

We have performed some calculations to test this method for calculating the dielectric properties of crystals. Therefore, we obtained the static and frequency-dependent dielectric function for the isotropic crystals of diamond (C), silicon (Si), and gallium arsenide (GaAs). The first two have the diamond, and the third the zinc-blend lattice type. All calculations were performed within the ADF-BAND (Refs. 30,31) program. We made use of frozen cores and a hybrid valence basis set consisting of the numerical solutions of a free-atom Herman–Skillman (HS) program,[36] in combination with Slater-type one-center functions (STO). The spatial resolution of this basis is equivalent to a triple-zeta STO basis that is augmented with two polarization functions. This valence basis was orthogonalized to the core states. The free-atom effective potential was provided by the same HS program. For the evaluation of the Coulomb integrals we used a single auxiliary basis of STO functions to represent the deformation density in the ground-state calculation and the induced density in the response calculation.

All matrix elements were evaluated numerically using an efficient and accurate quadrature scheme.[30,37] The numerical integration scheme for the **k**-space integrals was varied and used from 5 to 175 symmetry-unique sample points in the irreducible wedge of the Brillouin zone. All results shown here were obtained using the Vosko-Wilk-Nusair parametrization of the LDA exchange-correlation potential, which was also used to derive the ALDA exchange-correlation kernel.

First we obtained the static value for the dielectric function for diamond, and we investigated the convergence behavior as a function of the **k**-space sampling. In Fig. 1 we show the results for diamond in the low-frequency range, which were obtained using various **k**-space sampling densities, together with the experimental data as obtained from Ref. 38. The highest sampling density with 175 points gave identical results as the calculation using 111 points. This graph clearly shows that the results depend strongly on the accuracy of the numerical integration in **k**-space. Whereas in general most methods typically yield an overestimation for the static value of about 10%, we find for diamond an underestimation of about 5% for our most accurate result. In Table I we summarize our results for the static values for C, Si, and GaAs, which were obtained using the **k**-space sampling of 111 points, and we compare them with other theoretical and experimental values. Our results are in good agreement with the experimental data, and are comparable to other calculations.

We have also investigated the Coulomb and exchange-correlation contributions to the self-consistent potential. In Fig. 2 we plot the results for Si in the low-frequency range, which were obtained using a **k**-space sampling of 34 points. The uncoupled result is obtained by setting $\delta\mathbf{v}_{\text{eff}}(\mathbf{r},\omega)=\mathbf{0}$, which yields the bare response of the Kohn-Sham system. The coupled results have been obtained with and without inclusion of the exchange-correlation contribution. By including only the Coulomb contribution in the SCF procedure, the static value drops by about 25% relative to the bare response, from 12.9 to 9.9. Similar shifts, though smaller in magnitude, have been obtained in the dielectric matrix methods.[7,8,16,28] Including the exchange-correlation contribution in the coupled response raises the value again, relative to the Coulomb-only value by 10%, to 10.9. We can conclude that both the Coulomb interaction and exchange-correlation effects contribute considerably to the dielectric response, and that they are in the order of about 10%–15%. We find no major qualitative changes in the frequency dependence of the dielectric function, due to the coupling.

In Figs. 3, 4, and 5 we show the real and imaginary parts of the frequency-dependent dielectric function for the three materials C, Si, and GaAs, and we compare them with the experimental data as obtained from Refs. 38 and 39. All results have been obtained by including the Coulomb interaction and exchange-correlation effects in the SCF procedure. We verified numerically that the real and imaginary parts form Kramers–Kronig pairs. The overall correspondence with experiment is quite good, in particular for the low-frequency ranges. The sharp features in the spectra are reasonably well reproduced, and can be attributed to the van Hove-type singularities in the joint-density of states, as obtained from the Kohn–Sham band structure. They appear at energies which are uniformly shifted downwards with respect to the experiments by, respectively, about 1.0, 0.5, and 0.4 eV for C, Si, and GaAs. The calculated absorption edges

TABLE I. Static dielectric constants for C, Si, and GaAs.

Solid	Experiment	This Work	Other theory	Method [a b c d]
C	5.67 [e]	5.4	5.90 [f]	DM,PP,PW,XC
			5.20-5.86 [g]	DM,PP,PW,QP
			5.5 [h]	DM,PP,LCGO,QP
			4.34 [i]	UR,FP,LCAO
			5.7 [j]	UR,EP,LCAO
Si	11.4 [k]	11.6	12.4-12.9 [l]	DFPT,PP,PW,XC
			12.7 [m]	DFPT,PP,PW,XC
			13.6 [n]	DFPT,PP,PW,XC
			12.05 [o]	DM,FP,LMTO,QP
			12.7 [p]	DM,PP,PW,XC
			12.9 [q]	DM,PP,PW,XC
			11.2 [r]	DM,PP,PW,QP
			12.8 [h]	DM,PP,LCGO,QP
			9.03 [i]	UR,FP,LCAO
			11.7 [s]	UR,PP,LCGO,QP
			12.0 [j]	UR,EP,LCAO
GaAs	10.8 [t]	10.8	12.3 [m,n]	DFPT,PP,PW,XC
			10.83 [o]	DM,FP,LMTO,QP
			10.2 [u]	DM,PP,PW,QP
			13.1 [h]	DM,PP,LCGO,QP
			11.21 [i]	UR,FP,LCAO
			10.9 [s]	UR,PP,LCGO,QP
			10.9 [j]	UR,EP,LCAO

[a]DFPT: Density Function Perturbation Theory, DM: Dielectric Matrix, UR: Uncoupled Response.
[b]FP: Full Potential, PP: Pseudopotential, EP: Empirical Potential.
[c]PW: Plane Wave, LMTO: Linearized Muffin-Tin Orbitals, LCAO: Linear Combination of Atomic Orbitals, LCGO: Linear Combination of Gaussian Orbitals.
[d]XC: Exchange-Correlation Effects, QP: Quasi-Particle Energy Shift.
[e]Reference 42.
[f]Reference 28.
[g]Reference 18.
[h]Reference 43.
[i]Reference 44.
[j]Reference 45.
[k]Reference 46.
[l]Reference 13.
[m]Reference 29.
[n]Reference 47.
[o]Reference 48.
[p]Reference7.
[q]Reference 28.
[r]Reference 8.
[s]Reference 49.
[t]Reference 50.
[u]Reference 51.

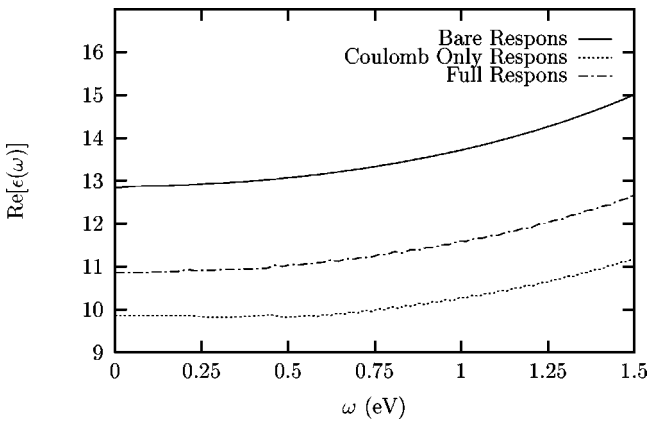

FIG. 2. The various contributions to the dielectric function of Si in the low-frequency range.

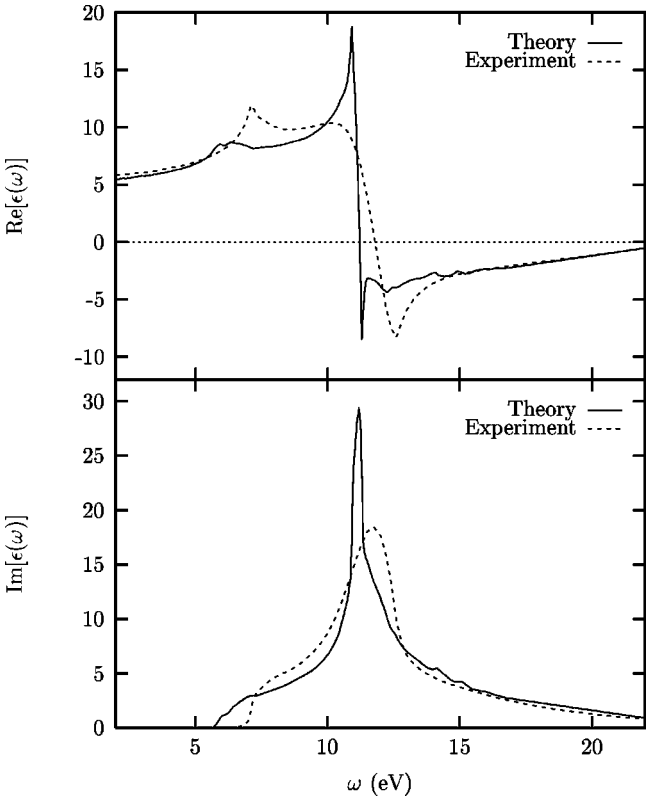

FIG. 3. Plots of the real and imaginary part of the calculated dielectric function of diamond (C) in comparison with the experimental data (Ref. 39).

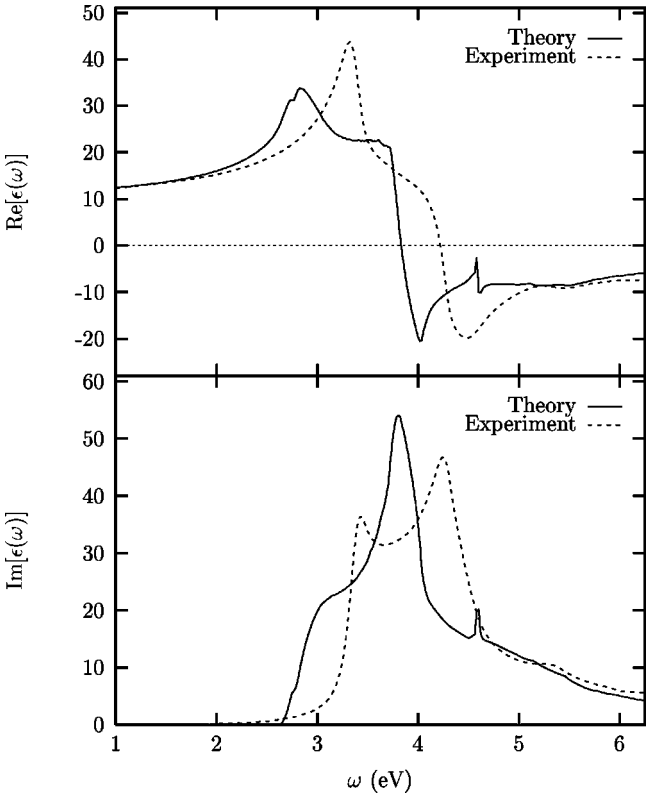

FIG. 4. Plots of the real and imaginary part of the calculated dielectric function of silicon (Si) in comparison with the experimental data (Refs. 38, 39).

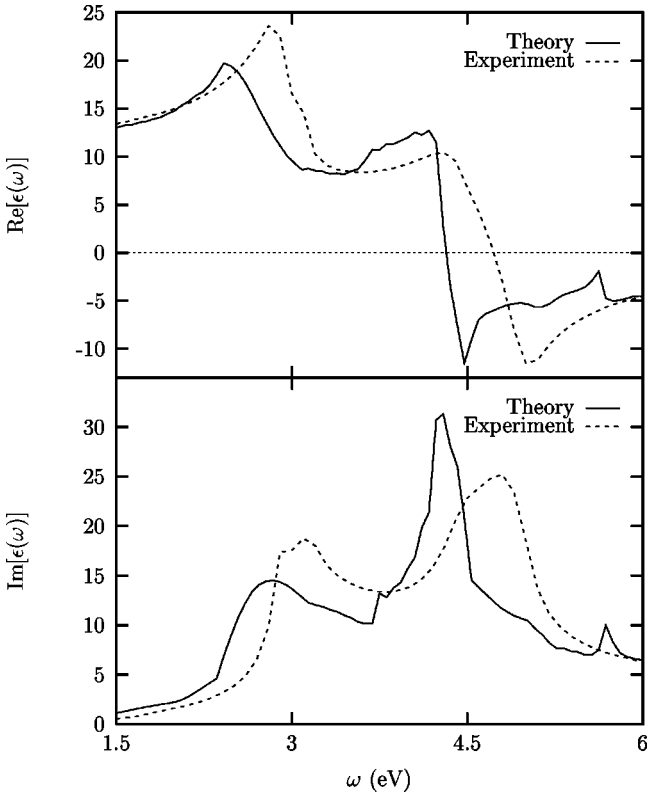

FIG. 5. Plots of the real and imaginary part of the calculated dielectric function of gallium arsenide (GaAs) in comparison with the experimental data (Ref. 39).

coincide with the vertical Kohn–Sham energy gap of, respectively, 5.6, 2.6, and 1.0 eV.

V. CONCLUSIONS

We have successfully applied time-dependent density functional theory to the dielectric response of nonmetallic crystalline systems. We used a perturbation approach to the time-dependent self-consistent field scheme, for which we derived a real-space description. This could only be achieved by combining a self-consistent lattice-periodic scalar potential with a uniform electric field. This field could be identified as the macroscopic electric field. In this description, exchange-correlation contributions and the microscopic Coulomb interactions were included in the self-consistent effective scalar potential. The macroscopic polarization and the electric susceptibility can then be obtained from the induced current density.

This method was implemented in a full-potential LCAO program. The coupled response can then be obtained with an efficiency that can be compared to ordinary DFT ground-state calculations. This high efficiency was achieved by using the space-group symmetry of the crystals, which led to the use of fully symmetric vector functions for the representation of the induced density and the SCF potential. The evaluation of Coulomb integrals was facilitated by using an auxiliary basis of vector functions to represent the density. This basis was constructed in such a way that the Coulomb integrals could be evaluated analytically. The lattice sums could be evaluated efficiently using a screening technique. The expensive, direct evaluation of the Kohn–Sham response kernels was avoided, and the singular integrals which appear in these kernels could be treated analytically.

We applied this method to obtain the dielectric function for the crystals of C, Si, and GaAs. The results show that Coulomb and exchange-correlation effects each contribute up to about 10%–15% of the coupled response. We obtained the static value and low-frequency range for the dielectric functions in good agreement with experiment. The frequency-dependent response reveals that spectral features appear at energies which coincide with the van Hove-type singularities in the bare Kohn–Sham response. The absorption edges can be found at the direct energy gap of the Kohn–Sham ground state band structure. The spectral features seem to be uniformly shifted downwards in energy by several tenths of an electron volt. However, a modification of the Kohn–Sham band structure by rigidly shifting the energies of the virtual states, (the scissors operator) seems not to be justified here. Such a procedure would affect the good agreement for the static value and low frequency range, even though it would correct the positions of the spectral features.

APPENDIX A: SCREENED POTENTIAL

An essential part of the screening technique is that the screened contribution of the uniform multipoles to the microscopic potential is uniform, i.e., not depending on the particular coordinate $\mathbf{r}$ at which the potential is evaluated. The screened instantaneous Coulomb potential $\delta v(\mathbf{r},t)$ of the uniform moments $\delta\mu^{(n)}(t)$ as needed in Eq. (11) is given by Eq. (7),

$$\delta v(\mathbf{r},t)=\lim_{c\to\infty}\sum_i h_c(|\mathbf{r}-\mathbf{R}_i|)\int_{V_i}\sum_{n=0}^{2}\frac{1}{n!}\delta\mu^{(n)}_{j_1\cdots j_n}(t)\cdot\frac{\partial^n}{\partial r'_{j_1}\cdots\partial r'_{j_n}}\frac{1}{|\mathbf{r}-\mathbf{r}'|}d\mathbf{r}', \tag{A1}$$

where a summation over all Cartesian components j_1 through j_n of the multipoles of rank n was implied. For notational convenience we will introduce the shorthand notation $\delta\mu^{(n)}\cdot\nabla'^{\,n}$ for this contraction. This potential can only be finite if $\delta\mu^{(0)}(t)=0$, i.e., if the uniform density vanishes identically. In the sequel we will only consider such cases.

As a first step, we will make the scale parameter c of the envelope function $h_c(|\mathbf{r}|)$ explicit. Let us therefore introduce the new scaled relative coordinates $\mathbf{x}=(\mathbf{r}-\mathbf{r}')/c$ and define also a much denser lattice (with an $\mathbf{r}$-dependent origin) by setting $\mathbf{X}_i=(\mathbf{r}-\mathbf{R}_i)/c$. The integration domains, i.e., the unit cells V_i map under this transformation to the $\mathbf{r}$-dependent $V_{i,\mathbf{r}}$. These $V_{i,\mathbf{r}}$ are the unit cells of the lattice defined by the $\mathbf{X}_i$. We will make a particular choice for the shape of the envelope function by setting $h_c(r)=h_1(r/c)$ for all c. For increasing c this envelope then only grows in size, but its shape remains the same. Application of this coordinate substitution yields the following expression

$$\delta v(\mathbf{r},t)=\lim_{c\to\infty}\sum_i h_1(|\mathbf{X}_i|)\int_{V_{i,\mathbf{r}}}\left(\sum_{n=1}^{2}\frac{(-c)^{2-n}}{n!}\delta\mu^{(n)}(t)\cdot\nabla^n\frac{1}{|\mathbf{x}|}\right)d\mathbf{x}. \tag{A2}$$

The singularity at $\mathbf{x}=0$ is integrable for $n\leqslant 2$. This formula reveals that the contribution of a multipole of rank n to the integrand scales like c^{2-n}. Somewhat hidden, though, is the c-dependence of the integration domain. However, naively replacing the summation and integration in the following way,

$$\lim_{c\to\infty}\sum_i h_1(|\mathbf{X}_i|)\int_{V_{i,\mathbf{r}}} g(\mathbf{x})d\mathbf{x}=\int h_1(|\mathbf{x}|)g(\mathbf{x})d\mathbf{x}, \tag{A3}$$

can only be justified for finite integrands $g(\mathbf{x})$. We will have to show that the corrugation, which is due to the evaluation of the envelope function at $\mathbf{r}$-dependent discrete lattice points $\mathbf{X}_i$ on one hand, and to the integration over the $\mathbf{r}$-dependent domains $V_{i,\mathbf{r}}$ on the other, vanishes in the limit. Let us include the $\mathbf{x}$-dependent part of the envelope in the integrand by using the following Taylor expansion around $\mathbf{x}\in V_{i,\mathbf{r}}$

$$h_1(|\mathbf{X}_i|)=\sum_{m=0}^{\infty}\frac{1}{m!}(\mathbf{X}_i-\mathbf{x})^m\cdot\nabla^m h_1(|\mathbf{x}|). \tag{A4}$$

The order of the general term in this Taylor series scales like $\mathcal{O}(|\mathbf{x}-\mathbf{X}_i|^m)=\mathcal{O}(c^{-m})$. Substitution gives

$$\delta v(\mathbf{r},t)=\lim_{c\to\infty}\sum_{n=1}^{2}\sum_{m=0}^{\infty}\frac{(-c)^{2-n-m}}{n!m!}\left(\sum_i\int_{V_{i,\mathbf{r}}}c^m(\mathbf{x}-\mathbf{X}_i)^m\cdot\nabla^m h_1(|\mathbf{x}|)\times\delta\mu^{(n)}(t)\cdot\nabla^n\frac{1}{|\mathbf{x}|}d\mathbf{x}\right). \tag{A5}$$

We will now show that the factor between brackets has a finite value for $c\to\infty$, so that all terms with $n+m>2$ vanish identically. Since the spacing of the lattice points $\mathbf{X}_i$ and the size of $V_{i,\mathbf{r}}$ will decrease for increasing c, the factor $c^m(\mathbf{x}-\mathbf{X}_i)^m$ will become an increasingly rapid fluctuating part of the integrand. It has the shape of a saw-tooth function with fixed extreme values. In the limit, only the average value of this fluctuating term is relevant, which can be separated from the rest according to

$$\lim_{c\to\infty}\sum_i\int_{V_{i,\mathbf{r}}}c^m(\mathbf{x}-\mathbf{X}_i)^m\cdot\nabla^m h_1(|\mathbf{x}|)\times\delta\mu^{(n)}(t)\cdot\nabla^n\frac{1}{|\mathbf{x}|}d\mathbf{x}$$
$$=\frac{1}{V_i}\int_{V_i}(\mathbf{r}'-\mathbf{R}_i)^m d\mathbf{r}'\cdot\int\nabla^m h_1(|\mathbf{x}|)\times\delta\mu^{(n)}(t)\cdot\nabla^n\frac{1}{|\mathbf{x}|}d\mathbf{x}. \tag{A6}$$

For $m=0$ this separation is trivial and already valid for arbitrary, finite, c. Here the first integral is over any one of the identical cells V_i. The second integral is over all space, and its value is finite for all m (and not depending on the particular coordinate $\mathbf{r}$), if we require all mth derivatives of the envelope to be regular in the origin and to fall off sufficiently fast for $|\mathbf{x}|\to\infty$. These demands can be met, by choosing, e.g., $h_1(x)=[1+\exp(\beta[x-1/x])]^{-1};\beta>0$, yielding a step-like function around $x=1$ with step width $1/\beta$, and a tail that falls off exponentially. Since it obeys the symmetry rule $h_1(x)=1-h_1(1/x)$ with $h_1(0)=1;h_1(\infty)=0$, it has the proper behavior at $x=0$ and $x=\infty$.

As argued above we have shown that all terms in Eq. (A5) with $n+m>2$ vanish in the limit. The terms with $n=0$ do not contribute since $\delta\mu^{(0)}(t)=0$, whereas the term with $n=1$, $m=0$ can be dropped (already for finite c) since the second integral in the right hand side of Eq. (A6) vanishes on symmetry grounds. All remaining terms have $m=2-n$, for which we obtain

$$\int\nabla^{2-n}h_1(|\mathbf{x}|)\otimes\nabla^n\frac{1}{|\mathbf{x}|}d\mathbf{x}=-(-1)^n\frac{4\pi}{3}1\quad(n=0,1,2). \tag{A7}$$

This result is not depending on the particular shape of the spherically symmetric screening function if it has the proper asymptotic behavior. These terms can merely lead to a uniform finite potential

$$\delta v(t)=\frac{4\pi}{3}\left(\delta\mu^{(1)}(t)\cdot\frac{1}{V}\int_V(\mathbf{r}-\mathbf{R})\,d\mathbf{r}-\frac{1}{2}\mathrm{Tr}(\delta\mu^{(2)}(t))\right). \tag{A8}$$

In conclusion, we get a uniform contribution $\delta v(t)$ to the microscopic potential due to the uniform multipoles if the unit cell is charge-neutral $\delta\mu^{(0)}=0$. This contribution has a value which does not depend on the particular shape of the spherically symmetric screening function.

APPENDIX B: QUADRATURE FOR RESPONSE KERNELS

The response integrals of Eq. (49) and Eq. (60) involve integrations over the irreducible wedge of the Brillouin zone, in which the denominator can become singular. A good way to treat these singularities is to use a Lehmann–Taut tetrahedron scheme,[40] in which the energy-dispersion relation of the denominator $\epsilon(\mathbf{k})=\epsilon_{a\mathbf{k}}-\epsilon_{i\mathbf{k}}$ is parametrized for each combination of i and a. We can separate the energy dependent part from the rest according to

$$I_{ia}(\omega)=\frac{1}{V_{\mathrm{IBZ}}}\int_{V_{\mathrm{IBZ}}}\frac{(f_{i\mathbf{k}}-f_{a\mathbf{k}})g(\mathbf{k})}{\omega-(\epsilon_{a\mathbf{k}}-\epsilon_{i\mathbf{k}})+i\eta}d\mathbf{k}=\int_{\epsilon_0}^{\epsilon_1}\frac{g_{ia}(\epsilon)}{\omega-\epsilon+i\eta}d\epsilon, \tag{B1}$$

where ϵ_0 and ϵ_1 are the minimum and maximum value of $\epsilon(\mathbf{k})$ occurring in V_{IBZ}. Since in nonmetallic systems the bands are either completely occupied or completely virtual, we can make the simplification $f_{i\mathbf{k}}-f_{a\mathbf{k}}=2$ and we get

$$g_{ia}(\epsilon)=\frac{2}{V_{\mathrm{IBZ}}}\int_{V_{\mathrm{IBZ}}}g(\mathbf{k})\,\delta(\epsilon-(\epsilon_{a\mathbf{k}}-\epsilon_{i\mathbf{k}}))\,d\mathbf{k}. \tag{B2}$$

For this integration accurate quadrature schemes exist (e.g., Ref. 41) which give us the weights $\tilde{w}_{ia\mathbf{k}_j}(\epsilon)$, such that

$$g_{ia}(\epsilon)=\sum_j \tilde{w}_{ia\mathbf{k}_j}(\epsilon)g(\mathbf{k}_j). \tag{B3}$$

In the linear tetrahedron scheme these weights are piecewise cubic polynomials in ϵ. For the quadrature of Eq. (50) we can write

$$I_{ia}(\omega)=\sum_j w_{ia\mathbf{k}_j}(\omega)g(\mathbf{k}_j). \tag{B4}$$

We only have to integrate the weights $\tilde{w}_{ia\mathbf{k}_j}(\epsilon)$ in the following way to obtain the new weights $w_{ia\mathbf{k}_j}(\omega)$ as functions of ω,

$$\begin{aligned} w_{ia\mathbf{k}_j}(\omega)&=\int_{\epsilon_0}^{\epsilon_1}\frac{\tilde{w}_{ia\mathbf{k}_j}(\epsilon)}{\omega-\epsilon+i\eta}d\epsilon \\ &=\mathcal{P}\int_{\epsilon_0}^{\epsilon_1}\frac{\tilde{w}_{ia\mathbf{k}_j}(\epsilon)}{\omega-\epsilon}d\epsilon+i\pi\,\tilde{w}_{ia\mathbf{k}_j}(\omega). \end{aligned} \tag{B5}$$

The real and imaginary parts of this weight can thus be obtained separately using the Cauchy principle value and residual parts.

APPENDIX C: SYMMETRY ADAPTED FITFUNCTIONS

For the efficient evaluation of the microscopic Coulomb potential we have to construct a basis of vector functions, which are orthogonal in the following sense:

$$\int \mathbf{f}_i(\mathbf{r})\cdot\mathbf{f}_j(\mathbf{r})\,d\mathbf{r}=\delta_{ij}, \tag{C1}$$

and which transform as totally-symmetric vector fields according to

$$\mathbf{f}_i(\mathbf{r})=\{\hat{\alpha}|\mathbf{t}_\alpha\}\mathbf{f}_i(\mathbf{r})=\alpha\cdot\mathbf{f}_i(\{\hat{\alpha}|\mathbf{t}_\alpha\}^{-1}\mathbf{r}). \tag{C2}$$

We can construct these fitfunctions as totally-symmetric Bloch sums of one-center functions $f_{nlm}(r)$,

$$f_{nlm}(\mathbf{r})=r^{n+l-1}\,\exp(-\zeta r)Z_{lm}(\hat{\mathbf{r}}). \tag{C3}$$

The $Z_{lm}(\hat{\mathbf{r}})$ are the real-valued spherical harmonics. In the actual fitset more than one value is used for the parameter ζ for each combination of n,l, and m. The Coulomb integrals of these one-center functions can be evaluated analytically using the following expansion of $1/|\mathbf{r}-\mathbf{r}'|$ in these spherical harmonics,

$$\frac{1}{|\mathbf{r}-\mathbf{r}'|}=\sum_{lm}\frac{4\pi}{2l+1}\frac{r_<^l}{r_>^{l+1}}Z_{lm}(\hat{\mathbf{r}})Z_{lm}(\hat{\mathbf{r}}'), \tag{C4}$$

where the $r_<$ and $r_>$ refer to the smaller and larger values, respectively, of the two radii r and r'. Using the orthogonality of the Z_{lm} functions we obtain

$$\begin{aligned} g_{nlm}(\mathbf{r})&=\int\frac{f_{nlm}(\mathbf{r}')}{|\mathbf{r}-\mathbf{r}'|}d\mathbf{r}' \\ &=\frac{4\pi}{2l+1}Z_{lm}(\hat{\mathbf{r}})\int_0^\infty\frac{r_<^l}{r_>^{l+1}}r'^{n+l+1} \\ &\quad\times\exp(-\zeta r')\,dr'. \end{aligned} \tag{C5}$$

This is again a one-center function of the same l and m value, but with a different radial dependence. The remaining integration over the radial coordinate r' can be evaluated easily. We can now construct the totally-symmetric Bloch sums of the fitfunctions $f_{nlm}(\mathbf{r})$ according to

$$\mathbf{f}_i(\mathbf{r})=\sum_{\{\hat{\alpha}|\mathbf{t}_\alpha\}\in\mathcal{G}}\{\hat{\alpha}|\mathbf{t}_\alpha\}f_{nlm}(\mathbf{r}-\mathbf{a})\,\mathbf{e}_\mu\,. \tag{C6}$$

The vectors $\mathbf{a}$ are the coordinates of the atoms in the irreducible wedge of the Wigner–Seitz cell, and $\mathbf{e}_\mu$ is a unit vector in either one of the Cartesian directions μ. For notational convenience we introduced the compound index $i=\{nlm,\mathbf{a},\mu\}$. Due to the operations $\{\hat{\alpha}|\mathbf{t}_\alpha\}$ of the crystal space group $\mathcal{G}$ this series develops into a linear combination of one-center functions with the same n and l values at equivalent atoms. The potential functions are constructed simultaneously, by using the screened Bloch sums of the one-center potential functions,

$$\mathbf{g}_i(\mathbf{r})=\sum_{\{\hat{\alpha}|\mathbf{t}_\alpha\}\in\mathcal{G}}\{\hat{\alpha}|\mathbf{t}_\alpha\}h_c(|\mathbf{r}-\mathbf{a}|)g_{nlm}(\mathbf{r}-\mathbf{a})\,\mathbf{e}_\mu\,. \tag{C7}$$

This set of functions is then orthogonalized by diagonalizing the (real and symmetric) overlap matrix of the vector fitfunctions $S_{ij}=\int\mathbf{f}_i(\mathbf{r})\cdot\mathbf{f}_j\,d\mathbf{r}$, i.e., by rewriting S in $S=ODO^T$ with O the orthogonal transformation matrix, and D a diagonal matrix. We only keep those elements j for which the diagonal elements d_j are larger than some threshold, and we obtain the orthogonalized set of fitfunctions $\mathbf{f}'_j(\mathbf{r})=d_j^{-1/2}\Sigma_i O_{ij}\mathbf{f}_i(\mathbf{r})$ and simultaneously we transform the potential functions accordingly to $\mathbf{g}'_j(\mathbf{r})=d_j^{-1/2}\Sigma_i O_{ij}\mathbf{g}_i(\mathbf{r})$.

The microscopic potential can only be defined for a neutral unit cell. Therefore, we have to do a constrained fit which automatically conserves charge. Using Eq. (54) we get

$$\begin{aligned} 0&=\int\delta\boldsymbol{\rho}(\mathbf{r},\omega)\,d\mathbf{r} \\ &=\int\sum_i c_i(\omega)\mathbf{f}'_i(\mathbf{r})\,d\mathbf{r} \\ &=\sum_i c_i(\omega)\int\mathbf{f}'_i(\mathbf{r})\,d\mathbf{r} \\ &=\sum_i c_i(\omega)\mathbf{n}_i\,, \end{aligned} \tag{C8}$$

in which the vectors $\mathbf{n}_i$ are the charge content of the fitfunctions

$$\mathbf{n}_i=\int\mathbf{f}'_i(\mathbf{r})\,d\mathbf{r}. \tag{C9}$$

This constraint results in three linear relations between the coefficients $c_i(\omega)$, one for each Cartesian component of the $\mathbf{n}_i$. We can minimize the fit error and implement the constraint by using the Lagrange multiplier technique. The set of Euler–Lagrange equations becomes

$$\frac{\partial}{\partial c_j}\left[\int \left|\delta\boldsymbol{\rho}(\mathbf{r},\omega)-\sum_i c_i(\omega)\mathbf{f}_i'(\mathbf{r})\right|^2 d\mathbf{r}+\boldsymbol{\lambda}(\omega)\cdot\sum_i c_i(\omega)\mathbf{n}_i\right]=0, \tag{C10}$$

which gives

$$-2v_j(\omega)+2c_j(\omega)+\boldsymbol{\lambda}(\omega)\cdot\mathbf{n}_j=0, \tag{C11}$$

where the $v_j(\omega)$ are obtained as the unconstrained fit coefficients

$$v_j(\omega)=\int \delta\boldsymbol{\rho}(\mathbf{r},\omega)\cdot\mathbf{f}_j'(\mathbf{r})\,d\mathbf{r}. \tag{C12}$$

Multiplying by $\mathbf{n}_j$, and summing over the indices j again, gives, after application of the constraint: $\Sigma_j c_j(\omega)\mathbf{n}_j=0$, the following equation

$$\left(\sum_j \mathbf{n}_j\otimes\mathbf{n}_j\right)\cdot\boldsymbol{\lambda}(\omega)=2\sum_j v_j(\omega)\mathbf{n}_j, \tag{C13}$$

which can be solved for $\boldsymbol{\lambda}(\omega)$ by inverting the 3×3 matrix $A=\Sigma_j\mathbf{n}_j\otimes\mathbf{n}_j$. The coefficients $c_i(\omega)$ then follow from this solution as

$$c_i(\omega)=v_i(\omega)-\frac{1}{2}\boldsymbol{\lambda}(\omega)\cdot\mathbf{n}_i. \tag{C14}$$

It is worthwhile to investigate if this constraint can be implemented during the construction of the fitfunctions, i.e., by making new linear combinations of them. The fitted density is obtained from Eq. (54) again, and, with the use of the expressions for the expansion coefficients Eq. (C14) and the solution for the multiplyers Eq. (C13), it takes the form

$$\delta\boldsymbol{\rho}(\mathbf{r},\omega)=\sum_i\left(v_i(\omega)-\frac{1}{2}\boldsymbol{\lambda}(\omega)\cdot\mathbf{n}_i\right)\mathbf{f}_i'(\mathbf{r})$$

$$=\sum_{ij}\mathbf{f}_i'(\mathbf{r})(\delta_{ij}-\mathbf{n}_i\cdot A^{-1}\cdot\mathbf{n}_j)v_j(\omega). \tag{C15}$$

Substitution of the expression (C12) for $v_j(\omega)$ yields

$$\delta\boldsymbol{\rho}(\mathbf{r},\omega)=\int\sum_{ij}\mathbf{f}_i'(\mathbf{r})(\delta_{ij}-\mathbf{n}_i\cdot A^{-1}\cdot\mathbf{n}_j)\mathbf{f}_j'(\mathbf{r}')\cdot\delta\boldsymbol{\rho}(\mathbf{r}',\omega)\,d\mathbf{r}'. \tag{C16}$$

It directly becomes clear that by diagonalizing the real and symmetric matrix B, which is defined by its components $B_{ij}=\delta_{ij}-\mathbf{n}_i\cdot A^{-1}\cdot\mathbf{n}_j$, we get a new set of orthogonal fitfunctions. Note that B is idempotent, i.e., $B^2=B$, so that it can only have eigenvalues equal to 1 or 0. With $B=ODO^T$ the reduced set of functions is then obtained by defining $\mathbf{f}_i''(\mathbf{r})=d_i^{1/2}\Sigma_j O_{ji}\mathbf{f}_j'(\mathbf{r})$. In exactly the same way the corresponding potential functions are transformed. The density can then be fitted as

$$\delta\boldsymbol{\rho}(\mathbf{r},\omega)=\sum_i c_i'(\omega)\mathbf{f}_i''(\mathbf{r}), \tag{C17}$$

where the fitcoefficients $c_i'(\omega)$ can be found as in an unconstrained fit from the relation

$$c_i'(\omega)=\int \delta\boldsymbol{\rho}(\mathbf{r},\omega)\cdot\mathbf{f}_i''(\mathbf{r})\,d\mathbf{r}. \tag{C18}$$

[1] P. Hohenberg and W. Kohn, Phys. Rev. B **136**, 864 (1964).
[2] W. Kohn and L. J. Sham, Phys. Rev. A **140**, 1133 (1965).
[3] R. O. Jones and O. Gunnarsson, Rev. Mod. Phys. **61**, 669 (1980).
[4] E. J. Baerends, D. E. Ellis, and P. Ros, Chem. Phys. **2**, 41 (1973).
[5] R. M. Dreizler and E. K. U. Gross, *Density Functional Theory; An Approach to the Quantum Many-Body Problem* (Springer Verlag, Berlin, 1990).
[6] R. G. Parr and W. Yang, *Density Functional Theory of Atoms and Molecules* (Oxford University Press, Oxford, 1990).
[7] S. Baroni and R. Resta, Phys. Rev. B **33**, 7017 (1986).
[8] Z. H. Levine and D. C. Allan, Phys. Rev. B **43**, 4187 (1991); **44**, 12781 (1991); Phys. Rev. Lett. **63**, 1719 (1989); **66**, 41 (1991).
[9] A. Zangwill and P. Soven, Phys. Rev. A **21**, 1561 (1980).
[10] R. van Leeuwen and E. J. Baerends, Phys. Rev. A **49**, 2421 (1994).
[11] S. J. A. van Gisbergen, V. P. Osinga, O. V. Gritsenko, R. van Leeuwen, J. G. Snijders, and E. J. Baerends, J. Chem. Phys. **105**, 3142 (1996).
[12] M. S. Hybertsen and S. G. Louie, Phys. Rev. B **30**, 5777 (1984).
[13] A. Dal Corso, S. Baroni, and R. Resta, Phys. Rev. B **49**, 5323 (1994).
[14] L. J. Sham and M. Schlüter, Phys. Rev. Lett. **51**, 1888 (1983); Phys. Rev. B **32**, 3883 (1965).
[15] J. P. Perdew and M. Levy, Phys. Rev. Lett. **51**, 1884 (1983).
[16] M. S. Hybertsen and S. G. Louie, Phys. Rev. B **34**, 5390 (1986).
[17] R. W. Godby, M. Schlüter, and L. J. Sham, Phys. Rev. Lett. **56**, 2415 (1986); Phys. Rev. B **37**, 10159 (1988).
[18] J. Chen, Z. H. Levine, and J. W. Wilkins, Phys. Rev. B **50**, 11514 (1994).
[19] X. Gonze Ph. Ghosez, and R. W. Godby, Phys. Rev. Lett. **74**, 4035 (1995).
[20] E. Runge and E. K. U. Gross, Phys. Rev. Lett. **52**, 997 (1984).
[21] G. D. Mahan and K. R. Subbaswami, *Local Density Theory of Polarizability* (Plenum, New York, 1990).
[22] E. K. U. Gross, C. A. Ullrich, and U. J. Gossmann, in *Density Functional Theory*, edited by E. K. U. Gross and R. M. Dreizler, (Plenum, New York, 1995), p. 149ff.
[23] S. J. A. van Gisbergen, J. G. Snijders, and E. J. Baerends, J. Chem. Phys. **103**, 9347 (1995); Comput. Phys. Commun. **118**, 119 (1999).
[24] A. K. Dhara and S.K. Ghosh, Phys. Rev. A **35**, 442 (1987).
[25] S. K. Ghosh and A. K. Dhara, Phys. Rev. A **38**, 1149 (1988).
[26] S. L. Adler, Phys. Rev. **126**, 413 (1962).
[27] N. Wiser, Phys. Rev. **129**, 62 (1963).
[28] M. S. Hybertsen and S. G. Louie, Phys. Rev. B **35**, 5585 (1987); **35**, 5602 (1987).
[29] S. Baroni, P. Giannozzi, and A. Testa, Phys. Rev. Lett. **58**, 1861 (1987).
[30] G. te Velde and E. J. Baerends, Phys. Rev. B **44**, 7888 (1991); J. Comput. Phys. **99**, 84 (1992).
[31] C. Fonseca Guerra, O. Visser, J. G. Snijders, G. te Velde, and E. J. Baerends, in *Methods and Techniques in Computational Chemistry*, edited by E. Clementi and G. Corongiu (STEF, Gagliary, 1995), p. 305.
[32] O. L. Brill and B. Goodman, Am. J. Phys. **35**, 832 (1967).
[33] G. Breit, Phys. Rev. **34**, 553 (1929); **39**, 616 (1932).
[34] S. H. Vosko, L. Wilk, and M. Nusair, Can. J. Phys. **58**, 1200 (1980).
[35] P. Pulay, Chem. Phys. Lett. **73**, 393 (1980); J. Comput. Chem. **3**, 556 (1982).
[36] F. Herman and S. Skillman, *Atomic Structure Calculations* (Prentice-Hall, Englewood Cliffs NJ, 1963).
[37] P. M. Boerrigter, G. de Velde, and E.J. Baerends, Int. J. Quantum Chem. **33**, 87 (1988).
[38] *Handbook of Optical Constants of Solids*, edited by E. D. Palik (Academic, New York, 1985).
[39] P. E. Aspnes and A. A. Studna, Phys. Rev. B **27**, 985 (1983).
[40] G. Lehmann and M. Taut, Phys. Status Solidi B **54**, 469 (1972).
[41] G. Wiesenekker and E. J. Baerends, J. Phys.: Condens. Matter **3**, 6721 (1991); G. Wiesenekker, G. te Velde, and E. J. Baerends, J. Phys. C **21**, 4263 (1988).

[42] *Numerical Data and Functional Relationships in Science and Technology*, edited by O. Madelung (Springer-Verlag, New York, 1982), Landolt-Börnstein, New Series, Group III, Vol. 17, Pt. A.
[43] M. Rohlfing, P. Krüger, and J. Pollmann, Phys. Rev. B **48**, 17791 (1993).
[44] M. Z. Huang and W. Y. Ching, Phys. Rev. B **47**, 9449 (1993).
[45] D. J. Moss, E. Ghahramani, J. E. Sipe, and H. M. van Driel, Phys. Rev. B **34**, 8758 (1986).
[46] H. H. Li, J. Chem. Phys. Ref. Data **9**, 561 (1980).
[47] P. Giannozzi, S. de Gironcoli, P. Pavone, and S. Baroni, Phys. Rev. B **43**, 7231 (1991).
[48] M. Alouani and J. Wills, Phys. Rev. B **54**, 2480 (1996).
[49] C. S. Wang and B. M. Klein, Phys. Rev. B **24**, 3417 (1981).
[50] K. B. Kahen and J. P. Leburton, Phys. Rev. B **32**, 5177 (1985).
[51] O. Pulci, G. Onida, A. I. Shkrebtii, R. Del Sole, and B. Adolph, Phys. Rev. B **55**, 6685 (1997).